Experimental and Theoretical Study of Strongly Focused High Intensity Ultrasound

V. Goland, L. Kushkuley, S. Mimran, Y. Zadok, S. Ben-Ezra, A. Shalgi, A. Rybianets
UltraShape Ltd., Yoqneam, Israel
E-male: vladimir@ultrashape.com

Abstract— **The model developed by the authors for strongly focused HIFU [2] was verified experimentally. The verification was performed for 1.03 MHz focusing transducer loaded by the water. The transducer comprised spherical piezo-element immersed in the mineral oil and had aperture diameter 84 mm. and focal radius 54 mm. At the first step, acoustic field distribution in a plane, which was close and parallel to the focal plane, was measured at 10 W of input electric power. Using this data, the normal velocity distribution over the plane which is tangent to the centre point of the spherical radiator was reconstructed. This distribution was further scaled and served as boundary conditions for calculation of high intensity field distribution using approach described in [2]. At the second step the model predictions were compared with the data extracted from the acoustical pressure waveforms measured for different values of the output acoustic power. In addition to usually extracted pressure harmonic content, the spatial distributions of harmonics of on-axis projection of particle velocity have been obtained from pressure harmonic distributions with the angle spectrum expansion, providing connection between pressure and particle velocity harmonics.**

The predictions of the pressure positive and negative peaks, harmonic content and dependence of the harmonic effective propagation angle on the harmonic number fitted closely the corresponding experimental results. The proposed approach allows accurate prediction of strongly focused HIFU fields based on the measurements of low-intensity field distributions.

Keywords: KZK equation, Westervelt equation, strongly focused high intensity ultrasound.

I. INTRODUCTION

Therapeutic ultrasound used for the treatment of subcutaneous tissues requires the application of strongly focused transducers which can create high intensity field within the target volume, yet not harming the surrounding tissues and the skin. As the half-aperture angle of focusing transducer grows, some of widely used theoretical models of HIFU, such as KZK equation, become invalid. To overcome the limitations of paraxial approximation a number of methods have been developed in the last decade. The one proposed in [1] allows accurate HIFU description for the half-aperture angles of focusing transducers up to 30-40 degrees. The approach developed in [2] has presumably a wider range of valid angles. It employs the concept of effective propagation angle which relates the amplitudes of pressure (divided by impedance) and on-axis projection of the particle velocity at focus. The goal of this work is to verify experimentally the model proposed in [2].

II. THEORY

The model developed in [2] is an asymptotic one-way propagation approximation of Westervelt equation:

$$(\Delta - \partial_{tt})p = -q\partial_{tt}(p^2),$$
$$q = \frac{P_0\beta}{\rho_0 c_0^2},\ \Delta = \Delta_\perp + \partial_{zz},\ \Delta_\perp = \partial_{xx} + \partial_{yy} \qquad (1)$$

Here β is a nonlinearity parameter, p, (x,y,z) and t are, respectively, dimensionless acoustical pressure, Cartesian coordinates and time, which are normalized by $P_o=u_o\rho_o c_o$, $k_o=2\pi f_o/c_o$ and $\omega_o=2\pi f_o$ correspondingly. The model describes an acoustic field radiated by focusing transducer which has radius of curvature F, aperture d, and is loaded by liquid having ambient sound speed c_o and density ρ_o. The surface of the radiator vibrates with the characteristic normal velocity amplitude u_o and frequency f_o in continue wave (CW) mode. Transducer acoustic axis is directed along z.

The CW solution of (1) can be expanded into Fourier series:

$$p(x,y,z,t) = \sum_{n=-\infty}^{\infty} p_n(x,y,z)\exp\left(-i\ n(t - z\cos\theta)\right) \qquad (2)$$

The effective angle θ introduced in (2) relates pressure and z-projection of particle velocity at focus $(p=u/\cos\theta)$ within the framework of the linear consideration. It is approximately $\sqrt{2}$ times less than the half aperture angle of a transducer. The truncated equations, which have been obtained in [2] from (1), describe the evolution of a finite set of pressure harmonics with respect to z coordinate:

$$\frac{\partial u_n}{\partial z} - i\left(\hat{l}_n - n\cos\theta\right)u_n - \alpha|n|^\mu u_n = -\frac{iqn}{2}\sum_{k=-N}^{N} p_k' p_{n-k}',$$
$$\hat{l}_n = \sqrt{n^2 + \Delta_\perp},\ \Delta_\perp = \frac{\partial^2}{\partial r^2} + \frac{1}{r}\frac{\partial}{\partial r}, \qquad (3)$$
$$p_k' = \begin{cases} p_k, & -N \le k \le N \\ 0, & otherwise \end{cases}$$

The phenomenological dissipation term is introduced into (3) to describe the power law of harmonics attenuation which is specified by the parameter μ. The substitution

$$u_n = p_n \cos\theta - \frac{i}{n}\frac{\partial p_n}{\partial z}, \qquad (4)$$

which has been used for obtaining (3) is the retarded coordinate *(τ=t-zcosθ)* version of linear connection between acoustic pressure and z-projection of particle velocity:

$$in\tilde{u}_n = \frac{\partial \tilde{p}_n}{\partial z} = i\hat{l}_n \tilde{p}_n,$$
$$(\tilde{u}_n, \tilde{p}_n) = (u_n, p_n)\exp(i\ nz\cos\theta) \qquad (5)$$

It has been noted in [2] that the local connection between u_n and p_n

$$p_n = \frac{u_n}{\cos\theta_n},\ \theta_n = \theta / n^{0.25} \qquad (6)$$

is approximately kept for weak shock waves as it follows from numerical simulations. The experimental verification of the connection is the one of main issues of the presented study.

Equations (3) can be solved using modified parabolic approximation proposed in [3]:

$$\hat{l}_n = n\cos\theta\left(1 + \frac{tg^2\theta}{2}\right) + \frac{\Delta_\perp}{2n\cos\theta},\ n > 0$$

along with the appropriate equivalent boundary condition and operator split method.

The procedure of the equivalent boundary condition formulation is composed of four steps. Firstly, the axially symmetric distribution of the complex pressure amplitude is extracted, as explained below, from a two-dimensional experimental scan of a low intensity pressure field over the plane $z = z'$ which is parallel to the focal plane and is separated from it by a distance of order of wave length. Then using this data, the distribution of *z*-projection of particle velocity over the focal plane is calculated with the integral formula [4]:

$$u(r,F) = \int_{S'} P(r',z') K_{pu}(|\vec{r} - \vec{r}'|, F - z')\ dx'dy'$$
$$\vec{r}' = (x', y'),\ \vec{r} = (x, y),\ K_{pu}(r,z) =$$
$$= \frac{i}{2\pi}\frac{\exp(iR)}{R^3}\left(\left(3 - R^2\right)\frac{z^2}{R^2} - 1 - iR\left(\frac{3z^2}{R^2} - 1\right)\right), \qquad (7)$$
$$K_{pu}(r, z<0) = K^*_{pu}(r, -z),\ R = \sqrt{r^2 + z^2}$$

At the third step, this distribution is recalculated with the modified Fresnel integral formula [3] into the normal velocity distribution over the plane z=0 which is tangent to the centre point of the spherical radiator:

$$u(r,0) = \int_{S'} u(r',F) K_{uu}(|\vec{r} - \vec{r}'|, -F)\ dx'dy',\ K_{uu}(r,z) =$$
$$= -\frac{ik_\theta}{2\pi z}\exp\left(ik_\theta\left(z\left(1 + \frac{1}{2}tg^2\theta\right) + \frac{r^2}{2z}\right)\right),\ k_\theta = \cos\theta \qquad (8)$$

Finally, the resulting distribution is scaled and serves as equivalent boundary conditions for (3). Since formulas (7), (8) have the form of two-dimensional convolution, a two-dimensional FFT algorithm is used for correspondent calculations.

In the case of a layered medium the described model is generalized as follows. The third step of the equivalent boundary condition formulation splits into the corresponding number of sub-steps. At the first sub-step, *z*-projection of particle velocity is recalculated with the modified Fresnel integral from the focal plane to the preceding interface. Then similar recalculation is fulfilled from one interface to another. The final sub-step will be the recalculation from the last interface to the Z=0 plane. Then the equations (3) are solved using acoustical parameters of the respective layer and condition of continuity for the velocity harmonics at the interfaces.

III. AXIALLY SYMMETRIC APPROXIMATION OF SCANNED DATA

Given the two-dimensional distribution of complex pressure amplitude, the axially symmetric approximation of the data can be obtained with the least square estimation method as follows.

Consider two-dimensional matrix $p_{ij} = p(i\Delta, j\Delta)$, *i=0,1,...,Nx-1, j=0,1,...,Ny-1*, where the spatial sampling interval Δ can be set to unit by choosing the corresponding measurement system.

Let the matrix p_{ij} have the following structure:

$$p_{ij} = P(r(i,j)) + \xi_{ij},$$
$$r(i,j) = \sqrt{(i - i_0)^2 + (j - j_0)^2} \qquad (9)$$

The indexes i_0, j_0 in (9) point to the center of approximate axial symmetry of the matrix p_{ij}, while the matrix ξ_{ij} describes the deviation of the original field from the axially symmetric field *P*. The function *P(r)* is assumed to have a first derivative within the interval of interest.

The objective is to find a sampled version of *P(r)* which satisfies the following condition:

$$\sum_{i=0}^{N_x-1}\sum_{j=0}^{N_y-1}\left(p_{ij} - p_{appr}(i,j)\right)^2 \Rightarrow \min \qquad (10)$$

The values $p_{appr}(i,j)$ in (10) have the form:

$$p_{appr}(i,j) = P_k + (P_{k+1} - P_k)(r(i,j) - k)$$

where $k = [r(i,j)]$. The sequence P_k is sought for *k=1,2,...,Nr-1*, where any integer number which is less than $\max_{i,j}[r(i,j)]$ can be chosen as the upper limit N_r-1 of the sequence. The first member of the sequence is defined as $P_0 = p_{i_0 j_0}$. The sequence is added by $P_{N_r} = 0$.

The set of the all pairs *(i,j)* which satisfy the condition $r(i,j) \le N_r - 1$ can be divided into $N_r - 1$ nonintersecting classes. Namely, the pair *(i,j)* belongs to the *k-th* class $((i,j) \in L_k)$ if and only if $k \le r(i,j) < k+1$. After this division, the criterion (10) will have the following form:

$$f(P_0, P_1, ..., P_{N_r-1}) \Rightarrow \min,\ f(P_0, P_1, ..., P_{N_r-1}) =$$

$$\sum_{k=0}^{N_r-2} \sum_{(i,j)\in L_k} \left(p_{ij} - P_k(1 - r(i,j) + k) - P_{k+1}(r(i,j) - k)\right)^2 \quad (11)$$

By differentiating (11) with respect to P_i, $i=1,2,...,N_r-1$, one can obtain a system of algebraic linear equations $\sum_{j=1}^{N_r-1} a_{ij} P_j = c_i$ having three-diagonal matrices a_{ij}:

$$a_{kk-1} = \sum_{(i,j)\in L_{k-1}} (k - r(i,j))(r(i,j) - k + 1)$$

$$a_{kk} = \sum_{(i,j)\in L_k} (k - r(i,j) + 1)^2 + \sum_{(i,j)\in L_{i-1}} (r(i,j) - k + 1)^2 \quad (12)$$

$$a_{kk+1} = \sum_{(i,j)\in L_k} (r(i,j) - k)(k - r(i,j) + 1)$$

The right part of the system has the form

$$c_k = \begin{cases} c'_k - a_{10} P_0, & i = 1 \\ c'_k, & i > 1 \end{cases},$$

$$c'_k = \quad (13)$$

$$\sum_{(i,j)\in L_{k-1}} p(i,j)(r(i,j) - k + 1) + \sum_{(i,j)\in L_k} p(i,j)(k - r(i,j))$$

Index *k* in (12) runs over the range (*1,2,...N_r*-1).

IV. Materials and Method

The experimental data was obtained for 1.03 MHz focusing transducer, which comprised spherical piezoelement having radius of curvature 54 mm and aperture diameter 84 mm (half aperture angle of 51 degrees). The piezoelement was sealed in the cylindrical housing filled with the mineral oil. The housing had an acoustic window made of very thin (0.15 mm) PVC membrane. The schematic transducer cross-section is shown in Fig.1

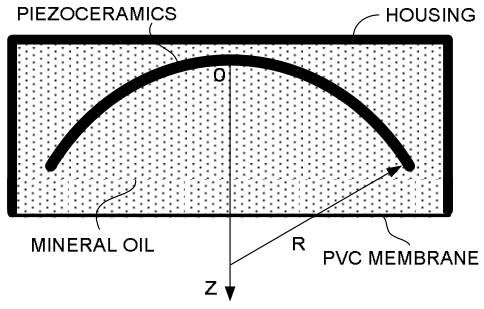

Fig.1 Schematic cross-section of the transducer

All measurements have been performed in NTR Acoustic Intensity Measurement System (AIMS), Onda Corp. For low and intermediate intensity field mapping we used NHR-0500 hydrophone (Onda Corp.). For high intensity fields a fiber-optic hydrophone (FOPH 2000, RP. Acoustics) was used. The transducer was loaded by the water. The excitation electric signal was generated by the arbitrary function generator Agilent 33220A and amplified by the power amplifier AG1021, T&C Power Conversion Inc. It had a form of a sinusoidal burst having duration of 60 μs and frequency 1.03 MHz.

The scan range was limited by the hydrophone sensitivity and was in the range $x, y \in [-10,10]$ mm. Its resolution was 0.2 mm. The approach for extracting the complex pressure amplitudes distribution from the recorded waveforms was based on the least square estimation of complex harmonics of quasi-periodic signals. This can be done using the FFT over the integer number of fundamental periods without any zero padding.

At the first step, low intensity acoustic pressure field distribution in the plane Z=58 mm was measured at 10.0 W electric input power (hereinbelow, the capital letters mean dimensional variables). Since, in general, measured field distributions are not axially symmetric, we used approach described in section III to symmetrize them. Further, based on symmetrical field distribution, the z-projection of velocity distribution in the focal plane (Z=54 mm) and then over the transducer-water interface plane (Z=40 mm) was reconstructed. Based on this distribution the normal velocity distribution in the plane Z=0, which is tangent to the centre point of the spherical radiator was reconstructed and scaled as it has been described above. Resulting data served as the equivalent boundary conditions for (3). At the second step the model predictions were compared with the data extracted from the acoustic pressure waveforms measured for different values of the total acoustic power.

In order to make the calculation of the equivalent boundary condition for nonlinear equations (3) more accurate, prior to reconstruction the two-dimensional distribution of the complex pressure amplitudes extracted from the scan were upsampled by factor 4 using the cubic spline interpolation.

V. Results and Discussion

In Fig. 2 is shown acoustic pressure signal in the focus at 127 W acoustic output. Both measured and predicted wave forms are plotted for comparison. Fig. 3, 4 present theoretical and experimental dependences of pressure harmonics and positive\negative peaks respectively on voltage amplitude applied to the transducer. The simulation was fulfilled with the following parameter settings: Oil - c_o=1390 m/s, ρ_o=835 kg m^{-3}, β_o=5.25, μ_o=1.7, α_o=7 neper m^{-1} at 1 MHz; water: c_1=1500 m/s, ρ_1=1000 kg m^{-3}, β_1=3.5, μ_1=2, α_o=0.025 neper m^{-1}@1 MHz.

In Fig. 5 and 6 are shown theoretical and experimental on-axis and radial (in the focal plane) distributions of the pressure for the first thee harmonics obtained at 17 W of the

total acoustic power. As one can see, the theoretical curves are pretty close to the experimental ones.

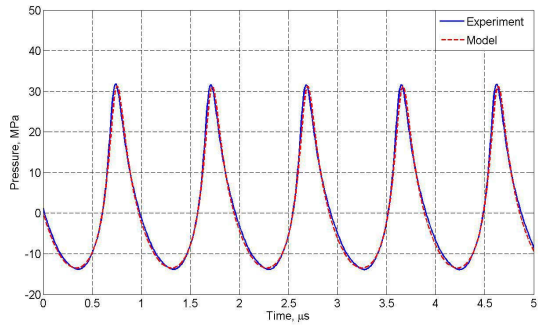

Fig. 2. Acoustic pressure in the focus for the total acoustic power 127 W.

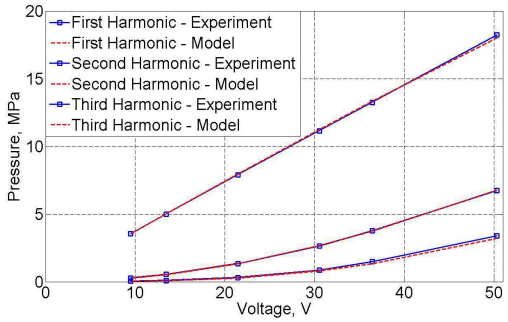

Fig.3 Dependence of the pressure in the focus on applied voltage amplitude for three first harmonics

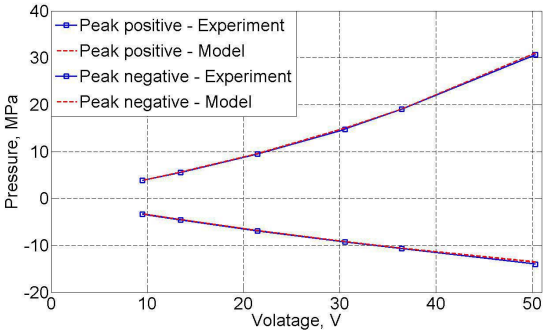

Fig.4 Dependence of the peak positive/negative pressure in the focus on applied voltage amplitude

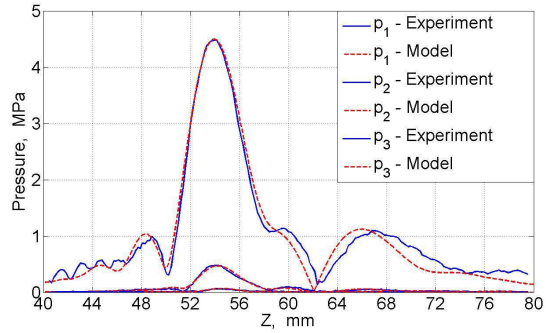

Fig.5 On-axis pressure distribution for the first three harmonics.

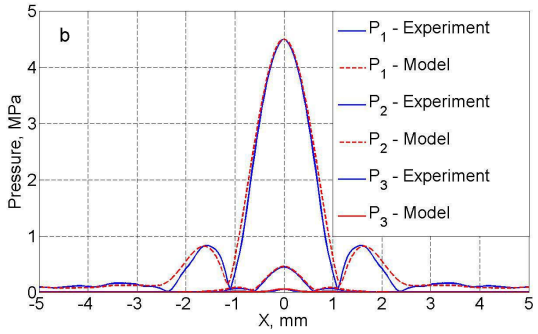

Fig.5 Radial pressure distribution for the first three harmonics.

Using equation (5) and experimental scan data for the pressure distribution in the focal plane we obtained a distribution of z components of particles velocity for the first three harmonics in this plane. The effective angles for each harmonic are calculated as $\theta_n = \arccos(u_n / p_n)$ and are presented in Table 1 together with the theoretical values. The experimental and theoretical results are fairly close one to another.

Table 1

Harmonic number	1	2	3
θ_n (theory)	36.10	30.36	27.43
θ_n (experiment)	36.16	30.67	28.05

The accounting of the connection between pressure and particle velocity of each harmonic is important, for example, for calculation of the heat deposition caused by the ultrasound energy dissipation. The standard approach based on the impedance connection between the pressure and particle velocity results in the significant overestimation of the heat deposition in the case of strongly focused field.

VI. Conclusion

The approach proposed in [2] allows accurate prediction of strongly focused HIFU fields based on the measurements of low-intensity field distributions.

References

[1] T. Kamakura, T. Ishiwata, K. Matsuda, "Model equation for strongly focused finite-amplitude sound beams," J. Acoust. Soc. Am. **107**, 3035-3046 (2000).

[2] V. Goland, Y. Eshel, L. Kushkuley, "Strongly curved short focus annular array for therapeutic applications," in Proceedings of the 2006 IEEE International Ultrasonics Symposium, pp. 2345-2348.

[3] V. Goland, M. Mogilevsky, Y. Eshel, L. Kushkuley, "Numerical simulation of finite-amplitude wave fields radiated by focusing ultrasonic transducer," WESPAC IX 2006.

[4] O. A. Sapozhnikov, Yu. A.Pishchal'nikov, and A.V. Morozov, "Reconstruction of the normal velocity distribution on the surface of an ultrasonic transducer from the acoustic pressure measured on a reference surface," Acoust. Phys. **49**, N3, 354-360 (2003).